

Argonne National Laboratory

THEORETICAL STUDY ON
THE TRANSFER FUNCTION OF BORAX-V
WITH CENTRAL SUPERHEATER

by

Jiro Wakabayashi

LEGAL NOTICE

This report was prepared as an account of Government sponsored work. Neither the United States, nor the Commission, nor any person acting on behalf of the Commission:

A. Makes any warranty or representation, expressed or implied, with respect to the accuracy, completeness, or usefulness of the information contained in this report, or that the use of any information, apparatus, method, or process disclosed in this report may not infringe privately owned rights; or

B. Assumes any liabilities with respect to the use of, or for damages resulting from the use of any information, apparatus, method, or process disclosed in this report.

As used in the above, "person acting on behalf of the Commission" includes any employee or contractor of the Commission, or employee of such contractor, to the extent that such employee or contractor of the Commission, or employee of such contractor prepares, disseminates, or provides access to, any information pursuant to his employment or contract with the Commission, or his employment with such contractor.

ARGONNE NATIONAL LABORATORY
9700 South Cass Avenue
Argonne, Illinois 60440

THEORETICAL STUDY ON
THE TRANSFER FUNCTION OF BORAX-V
WITH CENTRAL SUPERHEATER

by

Jiro Wakabayashi*

Idaho Division

August 1964

*Now at University of Kyoto, Kyoto, Japan

Operated by The University of Chicago
under
Contract W-31-109-eng-38
with the
U. S. Atomic Energy Commission

TABLE OF CONTENTS

	<u>Page</u>
NOMENCLATURE	6
ABSTRACT	7
I. ZERO-POWER REACTOR KINETICS	7
II. HEAT FLUX OF BOILING CORE	8
III. FUNDAMENTAL EQUATION OF MODERATOR DYNAMICS . .	11
IV. EFFECTS OF POWER VARIATIONS	12
A. Power-to-void Transfer Function	12
B. Power-to-boiling-boundary Transfer Function	15
V. PRESSURE-TO-VOID TRANSFER FUNCTION	18
VI. PRESSURE-TO-BOILING-BOUNDARY TRANSFER FUNCTION	20
VII. BOILING-BOUNDARY-TO-VOID TRANSFER FUNCTION . . .	21
VIII. HEAT-FLUX-TO-STEAM-MASS TRANSFER FUNCTION . . .	23
IX. STEAM-MASS-TO-PRESSURE TRANSFER FUNCTION	23
X. PRESSURE-TO-WATER-TEMPERATURE TRANSFER FUNCTION	24
XI. POWER-TO-WATER-TEMPERATURE TRANSFER FUNCTION FOR BOILER CORE	25
XII. POWER-TO-FUEL-TEMPERATURE TRANSFER FUNCTION FOR BOILING CORE	27
XIII. POWER-TO-FUEL-TEMPERATURE TRANSFER FUNCTION FOR SUPERHEATER CORE	28
XIV. NUMERICAL CONSTANTS, BLOCK DIAGRAM, AND ANALYTICAL RESULTS	32

TABLE OF CONTENTS

	<u>Page</u>
CONCLUSIONS.	38
ACKNOWLEDGMENT	39
REFERENCES.	40
SUPPLEMENTARY REFERENCES	40

LIST OF FIGURES

<u>No.</u>	<u>Title</u>	<u>Page</u>
2.1	Boiler-fuel Heat-transfer Parameters versus Biot Number for Cylindrical Geometry	10
14.1	Calculated Results for Various Natural-convection Flow Rates	32
14.2	System Block Diagram	33
14.3	Calculated Transfer Function at Various Power Levels; Natural Convection; Void Coefficient: $3.0 \times 10^{-3} \Delta k/\%$ Void. .	34
14.4	Calculated Transfer Function at Various Power Levels; Natural Convection; Void Coefficient: $4.5 \times 10^{-3} \Delta k/\%$ Void. .	35
14.5	Calculated Transfer Function at Various Power Levels; Forced Convection; 10,000 gpm; Void Coefficient: $3.0 \times 10^{-3} \Delta k/\%$ Void.	35
14.6	Calculated Transfer Function at Various Power Levels; Forced Convection; 10,000 gpm; Void Coefficient: $4.5 \times 10^{-3} \Delta k/\%$ Void.	36
14.7	Calculated Transfer Function at Various Flow Rates; Forced Convection; 20 MW; Void Coefficient: $3.0 \times 10^{-3} \Delta k/\%$ Void.	36
14.8	Calculated Transfer Function at Various Flow Rates; Forced Convection; 20 MW; Void Coefficient: $4.5 \times 10^{-3} \Delta k/\%$ Void.	37

TABLE OF CONTENTS

	<u>Page</u>
CONCLUSIONS.	38
ACKNOWLEDGMENT	39
REFERENCES.	40
SUPPLEMENTARY REFERENCES	40

Section I

C_i	Concentration of delayed neutrons emitted in group i
ΔK	Reactivity change
λ^*	Prompt neutron lifetime
N	Neutron density
N_0	Average neutron density
s	Laplace variable
t	Time
β	Effective delayed neutron fraction
β_i	Fraction of total neutrons emitted in group i
λ_i	Decay constant of delayed neutrons emitted in group i

Section II

F_i	Heat flux transfer function gain constants
H	Overall heat transfer coefficient of boiling core fuel rod
J_0, J_1	Bessel functions
N_b	Biot number for fuel
Q_b	Heat transfer rate to boiling water per unit length of rod
Q_b	Deviation in Q_b
Q_g	Heat generation rate of boiling core fuel rod per unit length
Q_g	Deviation in Q_g
R	Fuel rod radius
r	Fuel rod radial distance
T	Fuel characteristic time
γ	Fraction of heat flux transferred promptly to coolant
Θ_f	Fuel temperature
Θ_w	Water temperature
κ	Thermal diffusivity of boiler fuel pellet
λ	Thermal conductivity of boiler fuel pellet
τ_i	Heat flux transfer function time constants

Section III

A	$A_s + A_w$, or $A_{s0} + A_{w0}$
A_s	Cross-section area of steam per fuel rod
A_{s0}	Steady value of A_s
A_w	Cross-section area of water per fuel rod
A_{w0}	Steady value of A_w
a_s	Deviation of A_s in boiling core
a_w	Deviation of A_w in boiling core
h_s	Enthalpy of saturated steam
h_v	Volumetric heat capacity of saturated steam
h_w	Enthalpy of saturated water
h_s	Deviation in h_s
h_w	Deviation in h_w
P	Pressure of vessel
p	Deviation in P
U	Velocity of bubble
U_0	Steady value of U
u	Deviation in U
W	Velocity in water
W_0	Steady value of W
w	Deviation in W
x	Axial distance from bottom of fuel rod
ρ_s	Density of saturated steam
ρ_w	Density of saturated water

Section IV

a, b, c	Constants used in fitting the axial flux distribution; see Eq. (4.14)
d	Effective diameter of water channel
$D(x)$	Normalized, steady-state, axial flux distribution
E	Young's modulus of elasticity for stainless steel
e	Effective thickness of wall of water channel
g	Acceleration due to gravity

H_b	Effective height of bubble and water mixture
H_0	Enthalpy of subcooled water
h_0	Deviation in H_0
H_v	Volumetric heat capacity of saturated steam
K'	Bulk modulus of elasticity for stainless steel
L	Core height
L_b	Axial length from bottom to boiling boundary in the core
M_f	Mass flow rate of inlet water
\dot{M}_f	Water mass flow rate
q_b	Weighted heat transfer rate
\bar{U}_0	Average value of steam velocity (assumed constant)
\bar{v}_s	Weighted void volume deviation
$\bar{v}_s(s)$	Effective void cross-section deviation
δ	Deviation of boiling boundary
ρ_{sw}	Density of bubble and water mixture
τ_0	Bubble formation lag time
u	Velocity of pressure wave in bubble and water mixture

Section VI

H_{wf}	Enthalpy of feedwater
T_r	Recirculation time of water

Section VIII

$M_s(s)$	Total steam mass in the vessel
$m_s(s)$	Deviation in $M_s(s)$
$\dot{m}_s(s)$	Total rate of steam-mass variation
$\delta \dot{m}_s(s)$	Rate of steam-mass deviation for one fuel rod
n_b	Number of fuel rods in boiling core

Section IX

M_s	Total mass of steam inside the vessel
M_w	Total mass of water inside the vessel
θ_s	Saturated steam temperature

Section X

$\theta_w(s)$	Effective water temperature variation
---------------	---------------------------------------

Section XII

C_f	Heat capacity of boiling core fuel rod per unit length
-------	--

Section XIII

A_{ss}	Cross-section area of superheated steam per plate in superheater core
C_{sf}	Heat capacity of superheater core fuel plate per unit length
C_{ss}	Heat capacity (latent heat) of superheated steam at superheater core
h	Heat transfer coefficient of superheater core fuel plate per unit length
Q_{sf}	Heat generation rate of superheater fuel plate per unit length
q_{sf}	Deviation in Q_{sf}
U_{ss}	Velocity of superheated steam at superheater core
θ_{sf}	Temperature deviation of superheater fuel plate
θ_{ss}	Temperature deviation of superheated steam
ρ_{ss}	Density of superheated steam

Section XIV

K_{bi}	Fuel temperature coefficient of inner boiling core
K_{b0}	Fuel temperature coefficient of outer boiling core
K_{bs}	Fuel temperature coefficient of superheater core
K_{vi}	Void coefficient of inner boiling core
K_{v0}	Void coefficient of outer boiling core
$K_{\theta wi}$	Water temperature coefficient of inner boiling core
$K_{\theta w0}$	Water temperature coefficient of outer boiling core

Miscellaneous

Subscript i	Inner part of boiling core
Subscript 0	Outer part of boiling core
— (bar)	Spatially averaged value for a position

THEORETICAL STUDY ON THE TRANSFER FUNCTION OF BORAX-V WITH CENTRAL SUPERHEATER

by

Jiro Wakabayashi

ABSTRACT

An analytical, overall, reactor transfer function was derived to examine the stability problems of the BORAX-V boiling water reactor having an integral central superheater.

Special consideration was given to local pressure and time delay of void formation caused by superheating of the water. For this analysis, the boiling core was divided into inner and outer parts to introduce the effects of the radial flux distribution. Where appropriate, the analyses were individually done for these two boiler regions and the central superheater region, and the feedback effects were combined.

Basic assumptions introduced into the analyses are that (1) the flux deviation is proportional to the initial flux; (2) the power generation in the boiler (UO_2 pellets) and the superheater (UO_2 stainless steel cermet) is proportional to the overall reactor flux distribution; i.e., no spatial kinetic effects are considered; and (3) the individual reactivity phenomena (i.e., local temperature and void changes) are first-power flux-weighted to obtain the effective reactivity changes.

I. ZERO-POWER REACTOR KINETICS

The spatially-independent kinetic characteristics of a thermal reactor system are obtained by solving the following equations:

$$\frac{dN}{dt} = \left(\frac{\Delta K - \beta}{\ell^*} \right) N + \sum \lambda_i C_i; \quad (1.1)$$

$$\frac{dC_i}{dt} = \frac{\beta_i}{\ell^*} N - \lambda_i C_i, \quad i = 1, 2, \dots, 6. \quad (1.2)$$

If the above equations are combined and Laplace transformed, the zero-power transfer function is determined to be

$$\frac{\Delta N(s)/N_0}{\Delta K(s)} = \frac{1}{\ell^* s \left\{ 1 + \sum_{i=1}^6 \frac{\beta_i}{\ell^* (s + \lambda_i)} \right\}}; \quad (1.3)$$

and

$$\Delta K = \Delta K_{\text{ex}} + \Delta K_v + \Delta K_\theta + \Delta K_D, \quad (1.4)$$

where ΔK_{ex} is the externally inserted reactivity (of the control rods), and ΔK_v , ΔK_θ , and ΔK_D are, respectively, the reactivities due to void, water temperature, and fuel temperature (including the Doppler effect).

The values of constants λ_i , β_i , and ℓ^* are given on p. 32.

II. HEAT FLUX OF BOILING CORE

In the analyses of the heat flux from fuel rod to water coolant, it is assumed that the heat capacity of the cladding material is negligible with respect to that of the UO_2 pellets. The thermal conductivity of the cladding and the heat transfer coefficient from cladding to water are grouped as a single, overall, heat transfer coefficient, H .

The temperature in a power-generating medium of thermal conductivity, λ , and diffusivity, κ , is described as follows:⁽¹⁾

$$\nabla^2 \theta_f + \frac{Q_g}{\pi R^2 \lambda} = \frac{1}{\kappa} \cdot \frac{d\theta_f}{dt}, \quad (2.1)$$

where θ_f is the fuel temperature.

Since the fuel rod is essentially a cylinder of radius R , the boundary conditions are

$$\left. \frac{-d\theta_f}{dr} \right]_R = \frac{H}{\lambda} \left\{ \theta_f(R) - \theta_w \right\}, \quad (2.2)$$

$$\theta_f \neq \infty \text{ at } r = 0, \quad (2.3)$$

where θ_w is the water or boiling water temperature.

The temperature difference between the inlet water and the boiling water is negligible compared to that between the fuel surface and the boiling water. In the subcooling region, nucleate boiling also occurs on the surface of the cladding. Θ_w and H are assumed constant in all boiling regions.

Combining and Laplace transforming Eqs. (2.1) to (2.3) result in the following equations:

$$\Theta_f'(R,s) = \Theta_f'(R,s) - \Theta_w, \quad (2.4)$$

$$Q_b(s) = \Theta_f(R,s) 2\pi RH, \quad (2.5)$$

$$N_b \equiv RH/\lambda, \quad (2.6)$$

$$T \equiv R^3/\kappa, \quad (2.7)$$

and

$$Q_b(s) = Q_g(s) \left[\frac{2J_1 \sqrt{-Ts} / \sqrt{-Ts}}{J_0 \sqrt{-Ts} - \frac{\sqrt{-Ts}}{N_b} \cdot J_1 \sqrt{-Ts}} \right]. \quad (2.8)$$

Equation (2.8) may be expanded into the following series of partial fractions:

$$\frac{Q_b(s)}{Q_g(s)} = \sum_{i=1}^{\infty} \frac{F_i}{1 + \tau_i s}, \quad (2.9)$$

where boiler fuel heat, F_i and τ_i , are found from the simultaneous solution of

$$F_i = \frac{4\tau_i/T}{1 + T/\tau_i N_b^2}, \quad (2.10)$$

and

$$N_b = \sqrt{T/\tau_i} \left[\frac{J_1 \sqrt{T/\tau_i}}{J_0 \sqrt{T/\tau_i}} \right], \quad (2.11)$$

where J_0 and J_1 are Bessel functions.

As an approximation Eq. (2.9) may be rewritten as

$$\frac{Q_b}{Q_g} = \sum_{i=1}^3 \frac{F_i}{1 + \tau_{is}} + \frac{1 - \sum_{i=1}^3 F_i}{1 + \bar{\tau}_{4s}}, \quad (2.12)$$

where

$$\bar{\tau}_4 = \frac{\sum_{i=4}^{\infty} F_i \tau_i / T}{\sum_{i=4}^{\infty} F_i / T}. \quad (2.13)$$

Figure 2.1 gives the solution of Eqs. (2.10), (2.11), and (2.13) as a function of N_b .

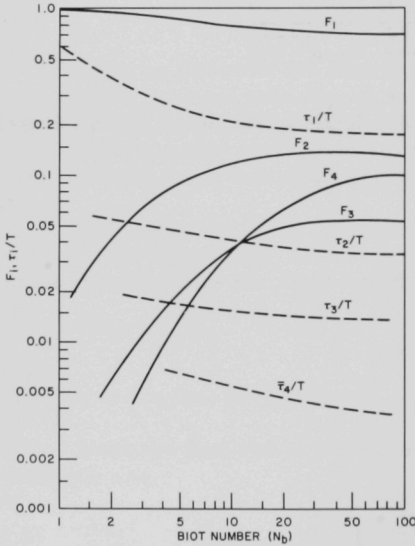


Fig. 2.1
Boiler-fuel Heat-transfer Parameters vs. Biot Number for Cylindrical Geometry

If it is assumed that the gamma energy release from the central superheater core is negligible, the power dissipated to the coolant (including γ , the gamma emission from the boiling core) is given by

$$\frac{Q_b(s)}{Q_g(s)} = \frac{q_b(s)}{q_g(s)} = (1 - \gamma) \left[\sum_{i=1}^3 \frac{F_i}{1 + \tau_i s} + \frac{1 - \sum_{i=1}^3 F_i}{1 + \tilde{\tau}_4 s} \right] + \gamma. \quad (2.14)$$

III. FUNDAMENTAL EQUATION OF MODERATOR DYNAMICS

The equations for conservation of mass and energy at the channel of a boiling core are

$$\frac{\partial(A_s \rho_s U + A_w \rho_w W)}{\partial x} + \frac{\partial(A_s \rho_s + A_w \rho_w)}{\partial t} = 0; \quad (3.1)$$

and

$$\frac{\partial(A_s H_s \rho_s U + A_w \rho_w H_w W)}{\partial x} + \frac{\partial(A_s H_s \rho_s + A_w H_w \rho_w)}{\partial t} = Q_b. \quad (3.2)$$

Since the values of $\partial H_s / \partial x$, $\partial H_w / \partial x$, and $\partial \rho_s / \partial x$ may be assumed to be zero, Eqs. (3.1) and (3.2) give

$$\frac{\partial A_s U}{\partial x} + \frac{\partial A_s}{\partial t} = \frac{Q_b}{(H_s - H_w) \rho_s} - \left[\frac{\rho_s A_s \frac{dH_s}{dp} + \rho_w A_w \frac{dH_w}{dp}}{(H_s - H_w) \rho_s} + \frac{A_s}{\rho_s} \cdot \frac{d\rho_s}{dp} \right] \frac{dP}{dt}. \quad (3.3)$$

If the deviations from the steady-state value are small compared to the steady-state value, Eq. (3.3) may be rewritten as

$$\frac{\partial}{\partial x} (a_s U_0 + u A_{s0}) + \frac{\partial a_s}{\partial t} = \frac{q_b}{H_v} - \left[\frac{1}{H_v} \left(\rho_s A_{s0} \frac{dH_s}{dp} + \rho_w A_{w0} \frac{dH_w}{dp} \right) + \frac{A_{s0}}{\rho_s} \cdot \frac{d\rho_s}{dp} \right] \frac{dP}{dt}, \quad (3.4)$$

where

$$H_v \equiv \rho_s (H_s - H_w), \quad (3.5)$$

and it is postulated that

$$a_s(x, t) U_0(x) + u(x, t) A_{s0}(x) \equiv U_p(x) a_s(x, t); \quad (3.6)$$

and

$$U_p(x) \equiv \zeta(x) U_0(x). \quad (3.7)$$

Since it was found that $\xi(x)$ approximates unity,⁽²⁾ Eq. (3.4) can be further simplified as

$$\frac{\partial U_0 a_s}{\partial x} + \frac{\partial a_s}{\partial t} = \frac{q_b}{H_v} - \left[\frac{1}{H_v} \left(\rho_s A_{s0} \frac{dH_s}{dp} + \rho_w A_{w0} \frac{dH_w}{dp} \right) + \frac{A_{s0}}{\rho_s} \cdot \frac{d\rho_s}{dp} \right] \frac{dP}{dt}. \quad (3.8)$$

IV. EFFECTS OF POWER VARIATIONS

The analysis of power-to-void transfer function is presented first in Section IVA, where the pressure and the boiling boundary are assumed constant. The power-to-boiling-boundary transfer function is derived in Section IVB.

If the transfer functions derived in Sections IV and VII are combined, the total effect of power changes on void is obtained.

A. Power-to-void Transfer Function

The following equation is obtained from Eq. (3.8) and includes the effect of the void transport across the core:

$$\frac{\partial U_0 a_s}{\partial x} + \frac{\partial a_s}{\partial t} = \frac{q_b(x,t)}{H_v}. \quad (4.1)$$

The initial and boundary conditions for solving Eq. (4.1) are

$$a_s(x,t) = 0 \quad \text{at } t = 0;$$

and

$$a_s(x,t) = 0 \quad \text{at } x = L_b.$$

In addition to the void transport effect described above, the void formation is delayed with respect to the heat flux deviation for several reasons. Because of the surface tension of the liquid, the pressure inside a bubble must be greater than the pressure of the water outside the bubble. Accordingly, energy must be spent for bubble formation. During bubble growth, the local water pressure rises and this pressure disturbance increases the saturation temperature of the water. The pressure again decreases with the transmission of the pressure wave into the void and water mixture. The void formation delayed is denoted as τ_0 , and the heat flux expended for the formation of steam is denoted as $q_b^1(x,t)$. If the bubble lag effect is included, the result is

$$\frac{\partial U_0 a_s}{\partial x} + s a_s = \frac{q_b^1(x,s)}{H_v}. \quad (4.2)$$

Equation (4.1) may be rewritten as follows:

$$q'_b(x,s) \equiv q_b(x,s)/(1+\tau_0 s). \quad (4.3)$$

The velocity of the pressure wave in the mixture of steam and water is

$$\omega = \frac{\sqrt{g \rho_{sw} K'}}{\sqrt{1 + (K'/E)d/e}}. \quad (4.4)$$

Since the value of $(K'/E)d/e$ is small compared to 1, Eq. (4.2) may be approximated as

$$\omega \cong \sqrt{g \rho_{sw} K'}. \quad (4.5)$$

The value of τ_0 may be estimated as

$$\tau_0 = H_e/\omega + 0.02. \quad (4.6)$$

The bubble formation lag is estimated to be between 10 and 30 msec. A value of 20 msec is used in this analysis.

If it is assumed that the position of the boiling boundary is not changed with time, $q'(x,s)$ may be denoted as

$$q'_b(x,s) \equiv \bar{q}'_b(s)D(x), \quad (4.7)$$

where $D(x)$ is the normalized, steady-state, axial flux distribution; i.e.,

$$\frac{1}{L} \int_0^L D(x) dx = 1. \quad (4.8)$$

Combining Eqs. (4.2) and (4.7) produces

$$\frac{dU_0 a_s(x,s)}{dx} + s a_s(x,s) = \frac{q'_b(s)}{H_v} D(x). \quad (4.9)$$

If the weighting function of void to reactivity, $F(x)$, is assumed equal to $D(x)/L$, the effective void cross-section deviation is

$$\bar{v}(s) = \int_{L_b}^L a(x,s) F(x) dx = \frac{1}{L} \int_{L_b}^L a(x,s) D(x) dx. \quad (4.10)$$

If Eq. (4.9) is solved for $a_s(x, s)$ and the result is substituted into Eq. (4.10), the following transfer function is obtained:

$$\frac{\bar{v}(s)}{\bar{q}_b'(s)} = \frac{1}{LH_v} \int_{L_b}^L D(x) dx \int_{L_b}^x D(x') e^{s\{t(x') - t(x)\}} dx', \quad (4.11)$$

and

$$\frac{\bar{v}(s)}{\bar{q}_b'(s)} = \frac{1}{1 + \tau_0 s} \cdot \frac{\bar{v}(s)}{\bar{q}_b'(s)}, \quad (4.12)$$

where

$$t(x) = \int_{L_b}^x \frac{1}{U_0(x)} dx. \quad (4.13)$$

Equation (4.12) is the general form of the power-to-effective-void, cross-section transfer function.

If the steam velocity, $U_0(x)$, is assumed to be a constant, \bar{U}_0 , and the normalized, axial flux distribution is denoted as

$$D(x) = a \sin(bx + c), \quad (4.14)$$

then Eq. (4.12) may be solved as follows:

$$\begin{aligned} \frac{\bar{v}(s)}{\bar{q}_b'(s)} &= \frac{1}{1 + \tau_0 s} \cdot \frac{a^2}{H_v \bar{U}_0} \int_{L_b}^L \sin(bx + c) dx \int_{L_b}^x \sin(bx' + c) e^{(s/\bar{U}_0)(x' - x)} dx \\ &= \frac{1}{1 + \tau_0 s} A_1 \left[\frac{B_1 + C_1 s + D_1 e^{-\tau_6 s}}{1 + \tau_5^2 s^2} + \frac{1 + e^{-\tau_6 s}(E_1 + F_1 s)}{(1 + \tau_5^2 s^2)^2} \right]; \end{aligned} \quad (4.15)$$

$$\frac{[\bar{v}(s)/A] \times 100}{\bar{q}_b'(s)} = \frac{100/A}{1 + \tau_0 s} \cdot A_1 \left[\frac{B_1 + C_1 s + D_1 e^{-\tau_6 s}}{1 + \tau_5^2 s^2} + \frac{1 + e^{-\tau_6 s}(E_1 + F_1 s)}{(1 + \tau_5^2 s^2)^2} \right], \quad (4.16)$$

where

$$A_1 = a^2 \tau_5 / (L_b H_v),$$

$$B_1 = \frac{1}{2} \left\{ \sin^2(bL + c) + \sin^2(bL_b + c) \right\},$$

$$C_1 = \tau_6/2 - (\tau_5/4) \{ \sin 2(bL + c) - \sin 2(bL_b + c) \},$$

$$D_1 = \sin(bL + c) \sin(bL_b + c),$$

$$E_1 = -\cos(\tau_6/\tau_5)$$

$$F_1 = -\tau_5 \sin(\tau_6/\tau_5)$$

$$\tau_5 = 1/(\bar{U}_0 b),$$

and

$$\tau_6 = b(L - L_b)/(\bar{U}_0 b) = b(L - L_b) \tau_5.$$

For simplicity, Eq. (4.16) is written as

$$(\bar{v}(s)/A) \cdot 100/\bar{q}_b(s) \cong [1/(1 + \tau_0 s)] \cdot [A_v/(1 + \tau_v s)], \quad (4.17)$$

where

$$A_v = (100/A) \cdot A_1(B_1 + D_1 + E_1 + 1),$$

$$\text{and } \tau_v = (B_1 + D_1 + E_1 + 1) \tau_5^2 / C_1.$$

B. Power-to-boiling-boundary Transfer Function

This section discusses the effect of power variations in the subcooled region of the core.

From Eq. (3.2), the following equation is valid for the subcooled region:

$$\frac{\partial(\rho_w A_w H_0 W_0)}{\partial x} + \frac{\partial(\rho_w A_w H_0)}{\partial t} = Q_b, \quad (4.18)$$

where $\rho_w A_w W_0$ is equal to the inlet water mass flow rate and ρ_w , A_w , and W_0 are assumed constant. Thus Eq. (4.18) can be rewritten as

$$\frac{\partial H_0}{\partial x} + \frac{1}{W_0} \frac{\partial H_0}{\partial t} = \frac{Q_b}{\dot{M}_f}. \quad (4.19)$$

Again, if only the transient parts are used (the steady-state values are subtracted), Eq. (4.19) becomes:

$$\frac{\partial h_0(x, t)}{\partial x} + \frac{1}{W_0} \frac{\partial h_0(x, t)}{\partial t} = \frac{q_b(x, t)}{\dot{M}_f}. \quad (4.20)$$

Initial and boundary conditions for solving Eq. (4.20) are

$$h_0(xt) = 0 \quad \text{at } t = 0;$$

and

$$h_0(xt) = 0 \quad \text{at } x = 0.$$

Using the Laplace transform method results in

$$\frac{dh_0(x,s)}{dx} + \frac{s}{W_0} h_0(x,s) = \frac{q_b(x,s)}{M_f}. \quad (4.21)$$

Then the solution of Eq. (4.21) is

$$M_f h_0(x,s) = \bar{q}_b(s) \int_0^x D(x') e^{(s/W_0)(x'-x)} dx'. \quad (4.22)$$

If the boiling boundary is denoted by δ , the following relation will be satisfied at any time (if h_0 is negative):

$$H_0(L_b + \delta) + h_0(L_b + \delta, t) = H_w = H_0(L_b). \quad (4.23)$$

If δ is small compared with L_b , the value of $h_0(L_b + \delta, t)$ can be replaced by $h_0(L_b, t)$.

From Eq. (4.19), the following equation is satisfied under steady-state conditions:

$$M_f \frac{dH_0(x)}{dx} = Q_b(x). \quad (4.24)$$

Now,

$$H_0(L_b + \delta) - H_0(L_b) = \frac{Q_b(L_b)}{M_f} \delta(t), \quad (4.25)$$

and in Eqs. (4.23) and (4.25), $\delta(t)$ is denoted as

$$\delta(t) = - [\dot{M}_f / Q_b(L_b)] h_0(L_b, t). \quad (4.26)$$

Equations (4.22) and (4.26) yield the following power-to-boiling-boundary transfer function:

$$\begin{aligned}
\frac{\delta(s)}{\bar{q}_b(s)} &= -\frac{1}{Q_b(L_b)} \int_0^{L_b} D(x) e^{-(s/W_0)(L_b-x)} dx \\
&= -\frac{a}{Q_b(L_b)b} \frac{\tau_7 s \sin(bL_b + c) - \cos(bL_b + c) - e^{-(L_b/W_0)s} \{\tau_7 s \sin c - \cos c\}}{1 + \tau_7^2 s^2} \\
&= A_2 \left[\frac{B_2 + C_2 s - e^{-\tau_7 s} (D_2 + E_2 s)}{1 + \tau_7^2 s^2} \right], \tag{4.27}
\end{aligned}$$

where

$$A_2 = -a/[Q_0(L_b)b],$$

$$B_2 = -\cos(bL_b + c),$$

$$C_2 = \tau_7 \sin(bL_b + c),$$

$$D_2 = -\cos c,$$

$$E_2 = \tau_7 \sin c,$$

and

$$\tau_7 = L_b/W_0.$$

For simplicity, Eq. (4.27) is written as

$$\frac{\delta(s)}{\bar{q}_b(s)} = \frac{A_\delta}{1 + \tau_\delta s}, \tag{4.28}$$

where

$$A_\delta = A_w(B_2 - D_2),$$

and

$$\tau_\delta = (B_2 - D_2)\tau_7^2/C_2.$$

V. PRESSURE-TO-VOID TRANSFER FUNCTION

In the analysis of the pressure-to-void transfer function, the power is assumed to remain constant. The following equation is obtained from Eq. (3.8):

$$\begin{aligned} \frac{\partial U_0 a_s}{\partial x} + \frac{\partial a_s}{\partial t} &= - \left[\frac{1}{H_v} \left(\rho_s A_{s0} \frac{dH_s}{dp} + \rho_w A_{w0} \frac{dH_w}{dp} \right) + \frac{A_{s0}}{\rho_s} \frac{d\rho_s}{dp} \right] \frac{dp}{dt} \\ &= -K(x) \frac{dp}{dt}. \end{aligned} \quad (5.1)$$

If the procedure used in solving Eq. (4.1) is followed, the solution of Eq. (5.1) is

$$\frac{\bar{v}(s)}{sp} = \frac{1}{1 + \tau_0 s} \int_{L_b}^L \frac{D(x)}{LU_0(x)} dx \int_{L_b}^x -K(x') e^{s\{t(x')-t(x)\}} dx'. \quad (5.2)$$

In Eq. (5.2), H_v , ρ_w , ρ_s , dH_s/dp , dH_w/dp , and $d\rho_s/dp$ are assumed constant. Since $A_{s0} + A_{w0} = A$ (the total channel cross section), a determination of A_{s0} is sufficient. $A_{s0}(x)$ is obtained by solving Eq. (3.3) at steady state. Thus,

$$\frac{d(A_{s0} U_0)}{dx} = \frac{Q_b(x)}{H_v}, \quad (5.3)$$

and

$$A_{s0}(x) = \frac{1}{H_v U_0(x)} \int_{L_b}^x Q_b(x') dx' = \frac{\bar{Q}_b}{H_v U_0(x)} \int_{L_b}^x D(x') dx'. \quad (5.4)$$

If $U_0(x)$ is again assumed constant, $A_{s0}(x)$ may be rewritten as

$$A_{s0}(x) = \frac{\bar{Q}_b a}{H_v \bar{U}_0 b} \{ \cos(bL_b + c) - \cos(bx + c) \}. \quad (5.5)$$

Substituting Eq. (5.5) into Eq. (5.1) results in

$$\begin{aligned} K(x) &= \frac{A \rho_w \left(\frac{dH_w}{dp} \right)}{H_v} \left[1 + \frac{Q_b a}{A \left(\frac{dH_w}{dp} \right) H_v \bar{U}_0 b} \cdot \left(\frac{dH_s}{dp} \cdot \frac{\rho_s}{\rho_w} - \frac{dH_w}{dp} + \frac{H_v}{\rho_s \rho_w} \cdot \frac{d\rho_s}{dp} \right) \right. \\ &\quad \left. \{ \cos(bL_b + c) - \cos(bx + c) \} \right] = \frac{\bar{U}_0}{a} K_1 - \frac{\bar{U}_0}{a} K_2 \cos(bx + c), \end{aligned} \quad (5.6)$$

where

$$K_1 = \frac{aA\rho_w \left(\frac{dH_w}{dp} \right)}{H_v \bar{U}_0} \left\{ 1 + \frac{\bar{Q}_{ba}}{A \left(\frac{dH_w}{dp} \right) H_v \bar{U}_0 b} \left(\frac{dH_s}{dp} \cdot \frac{\rho_s}{\rho_w} - \frac{dH_w}{dp} + \frac{H_v}{\rho_s \rho_w} \cdot \frac{d\rho_s}{dp} \right) \cdot \cos(bL_b + c) \right\}, \quad (5.7)$$

and

$$K_2 = \frac{aA\rho_w \left(\frac{dH_w}{dp} \right)}{H_v \bar{U}_0} \left\{ 1 + \frac{\bar{Q}_{ba}}{A \left(\frac{dH_w}{dp} \right) H_v \bar{U}_0 b} \left(\frac{dH_s}{dp} \cdot \frac{\rho_s}{\rho_w} - \frac{dH_w}{dp} + \frac{H_v}{\rho_s \rho_w} \cdot \frac{d\rho_s}{dp} \right) \right\}. \quad (5.8)$$

If Eq. (5.6) is substituted into Eq. (5.2), the pressure-to-void transfer function is

$$\begin{aligned} \frac{[\bar{v}(s)/A]100}{sp(s)} &= \frac{100/A}{1 + \tau_0 s} \cdot \frac{1}{L} \int_{L_b}^L \sin(bx + c) dx \int_{L_b}^x \{ -K_1 + K_2 \cos(bx' + c) \} e^{(S/\bar{U}_0)(x' - x)} dx', \\ &= \frac{1}{1 + \tau_0 s} \cdot \frac{100}{A} \left[\frac{A_3}{S} + \left\{ \frac{B_3 + C_3 s - e^{-\tau_0 s} (D_3 + E_3 s)}{1 + \tau_0^2 s^2} \right\} \right. \\ &\quad \left. \cdot \left\{ \frac{1}{s} - \frac{F_3 + G_3 s}{1 + \tau_0^2 s^2} \right\} + \frac{H_3 + I_3 s}{1 + \tau_0^2 s^2} \right], \end{aligned} \quad (5.9)$$

where:

$$\begin{aligned} A_3 &= [K_1/(b^2 \tau_0)] \{ \cos(bL + c) - \cos(bL_b + c) \}, \\ B_3 &= [K_1/(b^2 \tau_0)] \cos(bL_b + c), \\ C_3 &= (K_1/b^2) \sin(bL_b + c), \\ D_3 &= [K_1/(b^2 \tau_0)] \cos(bL + c), \\ E_3 &= (K_1/b^2) \sin(bL + c), \\ F_3 &= (K_2/K_1) \tau_0 \cdot \sin(bL_b + c), \\ G_3 &= (K_2/K_1) \tau_0^2 \cdot \cos(bL_b + c), \\ H_3 &= [K_2/(4b^2)] \{ 2b(L - L_b) - \sin 2(bL + c) + \sin 2(bL_b + c) \}, \end{aligned}$$

and

$$I_3 = [K_2/4b^2] \tau_5 \{ \cos 2(bL_b + c) - \cos 2(bL + c) \}.$$

For simplicity, Eq. (5.9) is written as

$$\frac{[\bar{v}(s)/A]100}{sp(s)} = \frac{1}{1 + \tau_0 s} \cdot \frac{A_{vp}}{1 + \tau_{vp} s},$$

where

$$A_{vp} = \{F_3(D_3 - B_3) + H_3 + C_3 - E_3 + \tau_6 D_3\} 100/A,$$

and

$$\tau_{vp} = \{F_3(D_3 - B_3) + H_3 + C_3 - E_3 + \tau_6 D_3\} / (I_3/\tau_5^2 + A_3).$$

(5.10)

VI. PRESSURE-TO-BOILING-BOUNDARY TRANSFER FUNCTION

Changes of pressure produce differences in the enthalpy of saturated water and consequently change the position of the boiling boundary.

From Eq. (4.24),

$$\dot{M}_f(H_w - H_{wf}) = \int_0^{L_b} Q_b(x) dx, \quad (6.1)$$

and the relation between the enthalpy of the water and the boiling boundary variation is as follows:

$$\dot{M}_f(H_w + h_w - H_{wf}) = \int_0^{L_b + \delta} Q_b(x) dx, \quad (6.2)$$

or

$$\dot{M}_f h_w = Q_b(L_b) \delta. \quad (6.3)$$

If the feedwater mass flowrate is negligible in comparison to that of the recirculation water, then the inlet water enthalpy will rise to $H_{wf} + h_w$ after recirculation time T_r . The pressure-to-boiling-boundary transfer function is therefore

$$\begin{aligned} \frac{\delta(s)}{sp(s)} &= \frac{dH_w}{dp} \cdot \frac{\dot{M}_f}{Q_b(L_b)} \cdot \frac{1 - e^{-sT_r}}{s} \\ &\approx \frac{dH_w}{dp} \cdot \frac{\dot{M}_f}{Q_b(L_b)} \cdot \frac{T_r}{1 + sT_r} = \frac{A_{\delta p}}{1 + sT_r}, \end{aligned} \quad (6.4)$$

where

$$A_{\delta p} = \frac{dH_w}{dp} \cdot \frac{\dot{M}_f}{Q_b(L_b)} \cdot T_r.$$

VII. BOILING-BOUNDARY-TO-VOID TRANSFER FUNCTION

The variation of the boiling boundary will cause variations in the volume of steam. The effect of the variation of steam production at the boiling boundary will appear at position x after transit time $t(x)$.

Including the bubble lag effect as derived in Section IV, the void formation variation of the boiling boundary can be denoted by

$$U_0(L_b) a_s(L_b, s) = -[Q_b(L_b) \delta(s)] / [H_v(1 + \tau_0 s)]. \quad (7.1)$$

Then the relation at any position x is

$$U_0(x) a_s(x, s) = -[Q_b(L_b) / H_v] \cdot [\delta(s) / (1 + \tau_0 s)] e^{-st(x)}. \quad (7.2)$$

From Eq. (4.7), the mean value of the effective void cross-section area deviation is given as

$$\bar{v}(s) = \frac{1}{L} \int_{L_b}^L a_s(x, s) D(x) dx. \quad (7.3)$$

If Eqs. (7.2) and (7.3) are combined, the boiling-boundary-to-void transfer function is

$$\frac{\bar{v}(s)}{\delta(s)} = - \frac{Q_b(L_b)}{H_v L} \cdot \frac{1}{1 + \tau_0 s} \int_{L_b}^L \frac{D(x)}{U_0(x)} e^{-st(x)} dx \quad (7.4)$$

$$= - \frac{Q_b(L_b)}{H_v L} \cdot \frac{1}{1 + \tau_0 s} \int_0^{T_s} D[x(t)] e^{-st} dt, \quad (7.5)$$

where

$$T_s = \int_{L_b}^L \frac{1}{U_0(x)} dx,$$

and

$$t = \int_{L_b}^{x(t)} \frac{1}{U_0(x')} dx'. \quad (7.6)$$

If the steam velocity is assumed constant, Eq. (7.5) becomes

$$\frac{\bar{v}(s)}{\delta(s)} = - \frac{Q_b(L_b)a}{H_v L} \cdot \frac{1}{1 + \tau_0 s} \int_0^{T_s} \sin(bU_0 t + bL_b + c) e^{-st} dt; \quad (7.7)$$

and

$$\frac{[\bar{v}(s)/A]100}{\delta(s)} = \frac{1}{1 + \tau_0 s} \cdot \frac{100}{A} \cdot A_4 \cdot \frac{B_4 + C_4 s - e^{-\tau_6 s}(D_4 + E_4 s)}{1 + \tau_5^2 s^2}; \quad (7.8)$$

where:

$$A_4 = - [Q_b(L_b)a\tau_1]/(H_v L),$$

$$B_4 = \cos(bL_b + c),$$

$$C_4 = \tau_5 \sin(bL_b + c),$$

$$D_4 = \cos(bL + c),$$

and

$$E_4 = \tau_5 \sin(bL + c).$$

For simplicity, Eq. (7.8) can be rewritten as

$$[\bar{v}(s)/A]100/\delta(s) = [1/(1 + \tau_0 s)] \cdot [A_{v\delta}/(1 + \tau_{v\delta}s)], \quad (7.9)$$

where

$$A_{v\delta} = A_4(B_4 - D_4),$$

and

$$\tau_{v\delta} = \tau_5^2(B_4 - D_4)/C_4.$$

VIII. HEAT-FLUX-TO-STEAM-MASS TRANSFER FUNCTION

As mentioned in Section IV, $q_b'(x, t)$ is the expenditure of energy for the formation of steam. The deviation of the steam formation rate $\delta \dot{m}_s(x, t)$ can be expressed as follows:

$$\delta \dot{m}_s(x, t) = q_b'(x, t) / (H_s - H_w), \quad (8.1)$$

or

$$\delta \dot{m}_s(x, s) = q_b(x, s) \cdot 1 / (1 + \tau_0 s) \cdot 1 / (H_s - H_w), \quad (8.2)$$

and

$$\begin{aligned} \delta \bar{m}(s) &= \frac{\bar{q}_b(s)}{H_s - H_w} \cdot \frac{1}{1 + \tau_0 s} \int_{L_b}^L D(x) dx \\ &= \frac{\bar{q}_b(s)}{H_s - H_w} \cdot \frac{1}{1 + \tau_0 s} \cdot \frac{a}{b} [\cos(bL_b + c) - \cos(bL + c)], \end{aligned} \quad (8.3)$$

where $\delta \bar{m}_s(s)$ is the rate of steam-mass variation for one fuel rod. The total rate of steam-mass variation, $\dot{m}_s(s)$, in the vessel is thus

$$\begin{aligned} \dot{m}_s(s) &= \frac{1}{1 + \tau_0 s} \cdot \frac{a}{(H_s - H_w)} \left[n_{bi} \bar{q}_{bi}(s) \{ \cos(bL_{bi} + c) - \cos(bL + c) \} \right. \\ &\quad \left. + n_{b0} \bar{q}_{b0}(s) \{ \cos(bL_{b0} + c) - \cos(bL + c) \} \right]. \end{aligned} \quad (8.4)$$

IX. STEAM-MASS-TO-PRESSURE TRANSFER FUNCTION

From Reference (3), the steam-mass-to-pressure transfer function is simplified to

$$\frac{sp(s)}{\dot{m}_s(s)} = \frac{1 + sT_r}{\eta \left(1 + s \cdot \frac{\gamma}{\eta} \cdot T_r \right)} = A_{pm} \cdot \frac{1 + T_r s}{1 + \tau_{pm} s}, \quad (9.1)$$

where

$$\left. \begin{aligned} \gamma &= \frac{M_s}{p} + \frac{M_s}{\theta_s} \cdot \frac{\partial \theta_s}{\partial p} + \frac{M_s \cdot \frac{\partial H_w}{\partial p}}{H_s - H_w}, \\ \eta &= \frac{M_s}{p} + \frac{M_s}{\theta_s} \cdot \frac{\partial \theta_s}{\partial p} + \frac{M_s \cdot \frac{\partial H_w}{\partial p}}{H_s - H_w} + \frac{M_w \cdot \frac{\partial H_w}{\partial p}}{H_s - H_w}, \end{aligned} \right\} \quad (9.2)$$

and

$$\begin{aligned} A_{pm} &= 1/\eta, \\ \tau_{pm} &= (\gamma/\eta) T_r. \end{aligned} \quad (9.3)$$

X. PRESSURE-TO-WATER-TEMPERATURE TRANSFER FUNCTION

The saturation temperature of the water in the boiling region is also changed by pressure variations. After the pressure deviation occurs, the core-inlet water temperature will change. This effect will appear in the nonboiling region after T_r seconds.

The effective water temperature variation is given by

$$\theta_w(s) = \frac{\partial \theta_w}{\partial p} \cdot \frac{p(s)}{L} \left[\int_{L_b}^L D(x) dx + e^{-sT_r} \cdot \int_0^{L_b} D(x) dx \right], \quad (10.1)$$

and the pressure-to-water-temperature transfer function becomes

$$\begin{aligned} \frac{\theta_w(s)}{p(s)} &= \frac{\partial \theta_w}{\partial p} \cdot \frac{a}{Lb} \left[\{\cos(bL_b + c) - \cos(bL + c)\} + e^{-sT_r} \{\cos c - \cos(bL_b + c)\} \right] \\ &\approx \frac{\partial \theta_w}{\partial p} \left[\frac{1 + sT_r \{\cos(bL_b + c) - \cos(bL + c)\} (a/bL)}{1 + T_r s} \right]. \end{aligned} \quad (10.2)$$

XI. POWER-TO-WATER-TEMPERATURE TRANSFER FUNCTION FOR BOILER CORE

As discussed in Section IV, some portion of the heat energy fluctuation in the boiling region is spent in superheating the water. From this it must be assumed that the water enthalpy in the boiling region can rise above the saturation enthalpy. In the nonboiling region, the effects of variation in heat flux on the temperature fluctuation do not include the effect of superheating of water.

If Eqs. (3.1), (3.2), (3.3), (3.4), and (4.4) are combined, the following equation for the boiling region results:

$$A_w \rho_w W \frac{\partial h_w}{\partial x} + A_w \rho_w W \frac{\partial h_w / W}{\partial t} = q_b - q_b^1. \quad (11.1)$$

The steam mass is negligible compared to the water mass; therefore, A_w , ρ_w and W are assumed constant. The enthalpy fluctuation, h_w , is proportional to the temperature fluctuation, θ_w . In this section, an average constant value of W is used (represented as \bar{W}). In addition, the subscript 1 refers to the boiling zone, and the subscript 2 refers to the subcooled zone. Thus, after Eq. (11.1) is Laplace transformed, the following equation can be written for the boiling zone:

$$\frac{\partial \theta_{w1}}{\partial x} + \frac{1}{\bar{W}} \cdot \frac{\partial \theta_{w1}}{\partial t} = K' q_b \cdot \frac{\tau_0 s}{1 + \tau_0 s}, \quad (11.2)$$

where

$$K' = K'' / (A_w \rho_w \bar{W}),$$

and

$$K'' = \theta_{w1} / h_w.$$

If the same procedure as the one in Section IV is used, the following transfer function is obtained:

$$\begin{aligned} \frac{\theta_{w1}(s)}{\bar{q}_b(s)} &= \frac{K'}{L \bar{W}} \cdot \frac{\tau_0 s}{1 + \tau_0 s} \int_{L_b}^L D(x) dx \int_{L_b}^x D(x') e^{(s/\bar{W})(x' - x)} dx' \\ &= \frac{\tau_0 s}{1 + \tau_0 s} \cdot A_5 \left[\frac{B_5 + C_5 s + D_5 e^{-\tau_9 s}}{1 + \tau_8^2 s^2} + \frac{1 + e^{-\tau_9 s} (E_5 + F_5 s)}{(1 + \tau_8^2 s^2)^2} \right], \end{aligned} \quad (11.3)$$

where

$$\begin{aligned}
 A_5 &= K' a^2 \tau_8 / L_b^2, \\
 B_5 &= -\frac{1}{2} \{ \sin^2(bL + c) + \sin^2(bL_b + c) \}, \\
 C_5 &= \tau_8 / 2 - (\tau_8 / 4) \{ \sin 2(bL + c) - \sin 2(bL_b + c) \}, \\
 D_5 &= \sin(bL + c) \sin(bL_b + c), \\
 E_5 &= -\cos(\tau_9 / \tau_8) \\
 F_5 &= -\tau_8 \sin(\tau_9 / \tau_8) \\
 \tau_8 &= 1 / \sqrt{W} b,
 \end{aligned}$$

and

$$\tau_9 = b(L - L_b) / \sqrt{W} b = b(L - L_b) \tau_8.$$

For simplicity, Eq. (11.3) is stated as

$$\frac{\theta_{w1}(s)}{q_b(s)} \cong \frac{\tau_0 s}{1 + \tau_0 s} \cdot \frac{A_{\theta q1}}{1 + \tau_{\theta q1} s}, \quad (11.4)$$

where

$$A_{\theta q1} = A_s (B_5 + D_5 + E_5 + 1),$$

and

$$\tau_{\theta q1} = (B_5 + D_5 + E_5 + 1) \tau_8^2 / C_5.$$

At the nonboiling region, Eq. (11.2) becomes

$$\frac{\partial \theta_{w2}}{\partial x} + \frac{1}{W_0} \cdot \frac{\partial \theta_{w2}}{\partial t} = K' q_b. \quad (11.5)$$

If the same procedure as the one above is used, the following transfer function is obtained:

$$\begin{aligned}
 \frac{\theta_{w2}(s)}{q_b(s)} &= \frac{K'}{LW_0} \int_0^{L_b} D(x) dx \int_0^x D(x') e^{(s/W_0)(x' - x)} dx', \\
 &= A_6 \left[\frac{B_6 + C_6 s + D_6 e^{-\tau_{11} s}}{1 + \tau_{10}^2 s^2} + \frac{1 + e^{-\tau_{11} s} (E_6 + F_6 s)}{(1 + \tau_{10}^2 s^2)^2} \right], \quad (11.6)
 \end{aligned}$$

where

$$A_6 = K'a^2 \tau_6 / (L_b^2),$$

$$B_6 = -\frac{1}{2} \{ \sin^2(bL_b + c) + \sin^2 c \},$$

$$C_6 = \tau_{11}/2 - (\tau_{10}/4) \{ \sin 2(bL_b + c) - \sin 2c \},$$

$$D_6 = \sin(bL_b + c) \sin c,$$

$$E_6 = -\cos(\tau_{11}/\tau_{10})$$

$$F_6 = -\tau_{10} \sin(\tau_{11}/\tau_{10})$$

$$\tau_{10} = 1/W_0 b,$$

and

$$\tau_{11} = bL_b/W_0 b = bL_b \tau_{10}.$$

For simplicity, Eq. (11.6) is written as

$$\frac{\theta_{w2}(s)}{\bar{q}_b(s)} \simeq \frac{A_{\theta q2}}{1 + \tau_{\theta q2} s}, \quad (11.7)$$

where

$$A_{\theta q2} = A_6(B_6 + D_6 + E_6 + 1),$$

and

$$\tau_{\theta q2} = (B_6 + D_6 + E_6 + 1) \tau_{10}^2 / C_6.$$

XII. POWER-TO-FUEL-TEMPERATURE TRANSFER FUNCTION FOR BOILING CORE

The difference between heat generation and heat energy transferred to water accounts for the temperature deviation, θ_f , of a fuel rod, as follows:

$$C_f \frac{d\theta_f(x,t)}{dt} = [\bar{q}_g(t) - \bar{q}_b(t)] D(x). \quad (12.1)$$

If the Laplace transform method is used, the effective average fuel temperature deviation, $\bar{\theta}_f$, is determined as follows:

$$s \bar{\theta}_f(s) = \frac{\bar{q}_g(s) - \bar{q}_b(s)}{C_f L} \int_0^L \{D(x)\}^2 dx. \quad (12.2)$$

From Eq. (12.2),

$$\frac{\bar{\theta}_f(s)}{\bar{q}_g(s)} = \frac{\{1 - \bar{q}_b(s)/\bar{q}_g(s)\}a^2}{C_f L s} \left\{ \frac{L}{2} - \frac{\sin 2(bL+c) - \sin 2L}{4b} \right\}. \quad (12.3)$$

XIII. POWER-TO-FUEL-TEMPERATURE TRANSFER FUNCTION FOR SUPERHEATER CORE

Temperatures in the superheater core are analyzed in two regions: steam flow up and steam flow down (i.e., first pass and second pass). The transfer function is calculated by using average values of these two passes.

In the superheater core, the fuel temperature only has an effect on the reactivity. If the thermal resistance of the stainless steel cladding is neglected, fuel temperatures may be calculated from the following relations:

$$C_{sf} \frac{d\theta_{sfj}}{dt} = q_{sfj} - h(\theta_{sfj} - \theta_{ssj}), \quad (13.1)$$

$$A_{ss} C_{ssj} \rho_{ssj} \frac{\partial \theta_{ssj}}{\partial t} + A_{ss} C_{ssj} \rho_{ssj} U_{ssj} \frac{\partial \theta_{ssj}}{\partial x} = h(\theta_{sfj} - \theta_{ssj}), \quad (13.2)$$

where $j(= 1 \text{ or } 2)$ corresponds to the first and second passes.

The pressure drop in the superheater core is negligible and the mass flow rate of the superheated steam is assumed constant. Thus,

$$\bar{\theta}_{sf1}(s) = \frac{1}{L} \int_0^L \frac{\bar{q}_{sf}(s) D'(x)/h + \theta_{ss1}}{1 + \tau_{12}s} D'(x) dx, \quad (13.3)$$

and

$$\bar{\theta}_{sf2}(s) = \frac{1}{L} \int_0^L \frac{\bar{q}_{sf}(s) D(x)/h + \theta_{ss2}}{1 + \tau_{12}s} D(x) dx, \quad (13.4)$$

where

$$D'(x) = a \sin(bL + C - bx),$$

and

$$\tau_{12} = C_{sf}/h.$$

If the Laplace transform method is used, Eq. (13.2) is replaced by

$$\frac{d\theta_{ss1}(x,s)}{dx} + \left\{ \frac{s}{U_{ss1}} + \frac{(h\tau_{12}/K_{s1})s}{1 + \tau_{12}s} \right\} \theta_{ss1} = \frac{1}{1 + \tau_{12}s} \cdot \frac{\bar{q}_{sf1}(s)}{K_{s1}} D'(x), \quad (13.5)$$

and

$$\frac{d\theta_{ss2}(x,s)}{dx} + \left\{ \frac{s}{U_{ss2}} + \frac{(h\tau_{12}/K_{s2})s}{1 + \tau_{12}s} \right\} \theta_{ss2} = \frac{1}{1 + \tau_{12}s} \cdot \frac{\bar{q}_{sf2}(s)}{K_{s2}} D(x), \quad (13.6)$$

where

$$K_{s1} = A_{ss} C_{ss1} \rho_{ss1} U_{ss1},$$

and

$$K_{s2} = A_{ss} C_{ss2} \rho_{ss1} U_{ss2}.$$

The solutions for $\theta_{ss1}(x,s)$ and $\theta_{ss2}(x,s)$ are as follows:

$$\theta_{ss1}(x,s) = \frac{\bar{q}_{sf1}(s)}{(1 + \tau_{12}s)K_{s1}} \int_0^x D'(x') e^{\{t'(x') - t'(x)\}} dx' + \theta_{ss1in}, \quad (13.7)$$

and

$$\theta_{ss2}(x,s) = \frac{\bar{q}_{sf2}(s)}{(1 + \tau_{12}s)K_{s2}} \int_0^x D(x') e^{\{t''(x') - t''(x)\}} dx' + \theta_{ss1}(L,s), \quad (13.8)$$

where

$$t'(x) = \int_0^x \left\{ \frac{s}{U_{ss1}} + \frac{(h\tau_{12}/K_{s1})s}{1 + \tau_{12}s} \right\} dx,$$

and

$$t''(x) = \int_0^x \left\{ \frac{s}{U_{ss2}} + \frac{(h \tau_{12}/K_{s2})s}{1 + \tau_{12}s} \right\} dx.$$

The temperature deviation of saturated steam, $\theta_{ss \text{ in}}$ (at the first pass inlet), is negligible. If the superheated steam velocities, U_{ss1} and U_{ss2} , are assumed constants, the transfer functions are

$$\begin{aligned} \frac{\bar{\theta}_{sf1}(s)}{\bar{q}_{sf}(s)} = \frac{1}{L} \int_0^L \left[\frac{1/h}{1 + \tau_{12}s} D'(x)^2 + \frac{D'(x)}{K_{s1}(1 + \tau_{12}s)^2} \int_0^x D'(x') \right. \\ \left. \cdot e^{\{t'(x') - t'(x)\}} dx' \right] dx, \end{aligned} \quad (13.9)$$

and

$$\begin{aligned} \frac{\bar{\theta}_{sf2}(s)}{\bar{q}_{sf}(s)} = \frac{1}{L} \int_0^L \left[\frac{1/h}{1 + \tau_{12}s} D(x)^2 + \frac{D(x)}{K_{s2}(1 + \tau_{12}s)^2} \int_0^x D(x') e^{\{t''(x') - t''(x)\}} dx' \right. \\ \left. + \frac{D(x) \theta_{ss1}(Ls)}{(1 + \tau_{12}s) \bar{q}_{sf}(s)} \right] dx, \end{aligned} \quad (13.10)$$

where

$$\begin{aligned} t'(x) = \alpha_1 s x = \left\{ \frac{1/U_{ss1} + \tau_{12}h/K_{s1} + (\tau_{12}/\bar{U}_{ss1})s}{1 + \tau_{12}s} \right\} s x \\ = (\beta_1 + \gamma_1 s) s x / (1 + \tau_{12}s), \end{aligned} \quad (13.11)$$

$$\begin{aligned} t''(x) = \alpha_2 s x = \left\{ \frac{1/U_{ss2} + \tau_{12}h/K_{s1} + (\tau_{12}/\bar{U}_{ss2})s}{1 + \tau_{12}s} \right\} s x \\ = (\beta_2 + \gamma_2 s) s x / (1 + \tau_{12}s), \end{aligned} \quad (13.12)$$

and

$$\frac{D(x) \theta_{ss1}(L, s)}{(1 + \tau_{12}s) \bar{q}_{sf}(s)} = \frac{D(x)}{(1 + \tau_{12}s)^2 K_{s1}} \int_0^L D'(x) e^{\{t'(x) - t'(L)\}} dx. \quad (13.13)$$

If $K_{s1} \simeq K_{s2}$, the transfer function for power generation rate to average superheater fuel temperature is

$$\begin{aligned}
\frac{\bar{\theta}_{sf}(s)}{\bar{q}_{fs}} &= \frac{\{\bar{\theta}_{sf1}(s) + \bar{\theta}_{sf2}(s)\}/2}{\bar{q}_{sf}(s)} \\
&= \frac{A_7}{1 + \tau_{12}s} + B_7 \left\{ \frac{C_7 + D_7s + e^{-\alpha_1 L s} (E_7 + F_7s)}{(1 + \tau_{12}s)^2 \left(1 + \frac{\alpha_1}{b^2} s^2\right)} \right. \\
&\quad \left. + \frac{G_7 + H_7s^2 + e^{-\alpha_1 L s} (I_7 + J_7s + K_7s^2)}{(1 + \tau_{12}s)^2 \left(1 + \frac{\alpha_1}{b^2} s^2\right)} \right\}, \tag{13.14}
\end{aligned}$$

where

$$\begin{aligned}
A_7 &= \frac{a^2}{H_S L} \left\{ \frac{L}{2} + \frac{\sin 2c - \sin 2(bL + c)}{4b} \right\}, \\
B_7 &= a^2 / (K_{S1} L b^2), \\
C_7 &= [\cos^2 c - \cos c \cos(bL + c)] / 2, \\
D_7 &= (\alpha_1 / b) \{ Lb / 2 + [2 \sin 2c - \sin 2(bL + c) - 2 \sin c \cos(bL + c)] / 4 \}, \\
E_7 &= [\cos^2(bL + c) - \cos c \cos(bL + c)] / 2, \\
F_7 &= (\alpha_1 / b) \{ \cos(bL + c) \sin(bL + c) - \cos c \sin(bL + c) \} / 2, \\
G_7 &= \{ \cos^2 c + \cos^2(bL + c) \} / 2, \\
H_7 &= -(\alpha_1^2 / 2b^2) \{ \sin^2 c + \sin^2(bL + c) \}, \\
I_7 &= -\cos c \cos(bL + c), \\
J_7 &= -(\alpha_1 / b) \sin bL,
\end{aligned}$$

and

$$K_7 = (\alpha_1^2 / b^2) \sin c \sin(bL + c).$$

For simplicity, Eq. (13.14) is written

$$\frac{\theta_{sf}(s)}{q_{sf}(s)} = \frac{A_S}{1 + \tau_{Ss}}, \tag{13.15}$$

where

$$A_S = A_7 + B_7(C_7 + E_7 + G_7 + I_7),$$

and

$$\tau_S = \tau_{12} \{ A_7 + B_7(C_7 + E_7 + G_7 + I_7) \} / A_7.$$

XIV. NUMERICAL CONSTANTS, BLOCK DIAGRAM, AND ANALYTICAL RESULTS

In the analysis presented here, the prompt neutron lifetime, ℓ^* , and the effective delayed neutron fraction, β , were assumed to be 2.7×10^{-5} and 0.0071, respectively. The remaining delayed neutron parameters are presented in Table 14.1.

Table 14.1

DELAYED NEUTRON PARAMETERS

i	λ_i	β_i
1	0.0129	0.000270
2	0.0317	0.001512
3	0.115	0.001335
4	0.311	0.002889
5	1.4	0.000909
6	3.88	0.000185

Experimentally, three cases of reactor operating modes were considered: 1) natural convection at various mean power levels; 2) forced convection (10,000 gpm) at various mean power levels; and 3) 20-MW mean power level with various forced-convection flow rates. The vessel pressure was assumed constant at 600 psi. For calculation of the forced-convection cases, a constant value of 1.5 was used for the slip ratio in the boiling channel. The flow rate of both water and steam versus boiler heat flux for the natural-convection core was calculated with the RECHOP Code⁽⁴⁾ as shown in Fig. 14.1. The core geometry is taken from ANL-6302⁽⁵⁾.

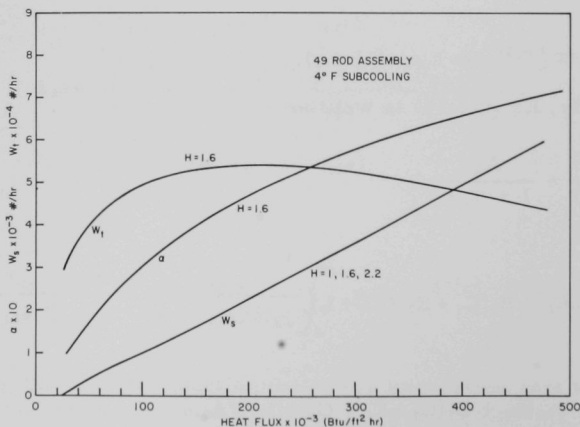


Fig. 14.1. Calculated Results for Various Natural-convection Flow Rates

Figure 14.2 is the resulting block diagram for the reactor system analyzed in this report, where α_1 , α_2 , and α_3 are the local-to-average power generation ratios in the inner boiler core, the outer boiler core, and the superheater core, respectively. Table 14.2 lists the physical constants used in the transfer functions derived above.

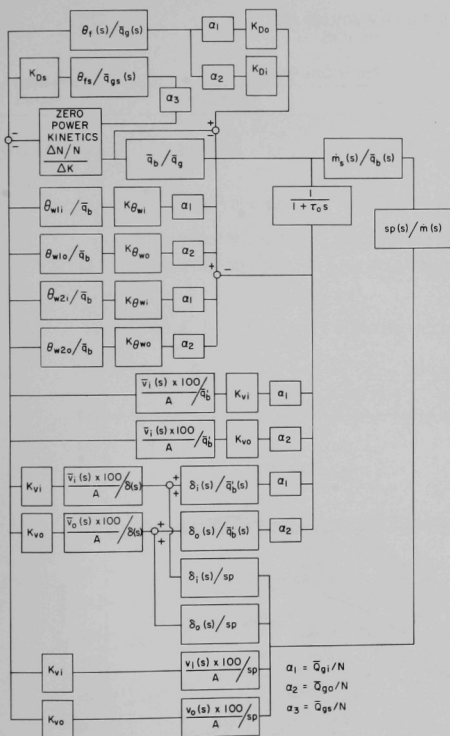


Fig. 14.2
System Block Diagram

Table 14.2

PHYSICAL CONSTANTS

λ (Btu/ft hr °F)	0.9	γ	0.03	$H_5 - H_w$ (Btu/lb)	732.58
K (ft ² /sec)	5.4×10^{-6}	Q_{gs}/Q_g	17/83	$\partial H_5/\partial p$ (Btu/psi-lb)	-0.01772
$H = \frac{1}{r + d_c/\lambda_c + 1/h_f}$ (Btu/ft ² hr °F)	1860	A (ft ²)	0.0012174	$\partial H_w/\partial p$ (Btu/psi-lb)	0.20755
r^* (ft hr °F/Btu)	0.0002	L (ft)	2	$\partial \rho_s/\partial p$ (lb/ft ³ -psi)	0.002247
d_c^{**} (ft)	0.00125	ρ_s (lb/ft ³)	1.2997	$\partial \theta_s/\partial p$ (°F/psi)	0.17845
λ_c^\dagger (Btu/ft hr °F)	7.45	ρ_w (lb/ft ³)	49.704	a	1.33637
h_f (Btu/ft ² hr °F)	6000	H_v (Btu/ft ³)	924.04	b	1.24
R (ft)	0.0143	M_w (lb)	8350	c	0.52576
		M_s (lb)	149		

* r : Thermal resistance of UO₂ pellet to cladding.

** d_c : Thickness of stainless steel cladding.

$\dagger \lambda_c$: Thermal conductivity of cladding.

This analysis was done for two assumed values of average void coefficients, using the average reactivity coefficients listed in Table 14.3. The ratio of the individual coefficients for the inner and outer boiling cores was assumed to equal the ratio of the mean neutron fluxes in these two regions.

Table 14.3
REACTIVITY COEFFICIENTS FOR BOILING AND
SUPERHEATING CORE REGIONS

	Average	Boiling Core Regions		Superheating Core Regions
		Inner Core	Outer Core	
Fuel temperature coefficient (Doppler)	$-1.8 \times 10^{-5} \Delta k / ^\circ F$	$-1 \times 10^{-5} \Delta k / ^\circ F$	$-0.8 \times 10^{-5} \Delta k / ^\circ F$	$-0.6 \times 10^{-5} \Delta k / ^\circ F$
Water temperature coefficient	$-1 \times 10^{-3} \Delta k / ^\circ F$	$-0.6 \times 10^{-3} \Delta k / ^\circ F$	$-0.4 \times 10^{-3} \Delta k / ^\circ F$	-
Void coefficient	$-3 \times 10^{-3} \Delta k / \% \text{ void}$	$-1.68 \times 10^{-3} \Delta k / \% \text{ void}$	$-1.32 \times 10^{-3} \Delta k / \% \text{ void}$	-
	$-4.5 \times 10^{-3} \Delta k / \% \text{ void}$	$-2.52 \times 10^{-3} \Delta k / \% \text{ void}$	$-1.98 \times 10^{-3} \Delta k / \% \text{ void}$	-

The analytical results are shown in Figs. 14.3 to 14.8.

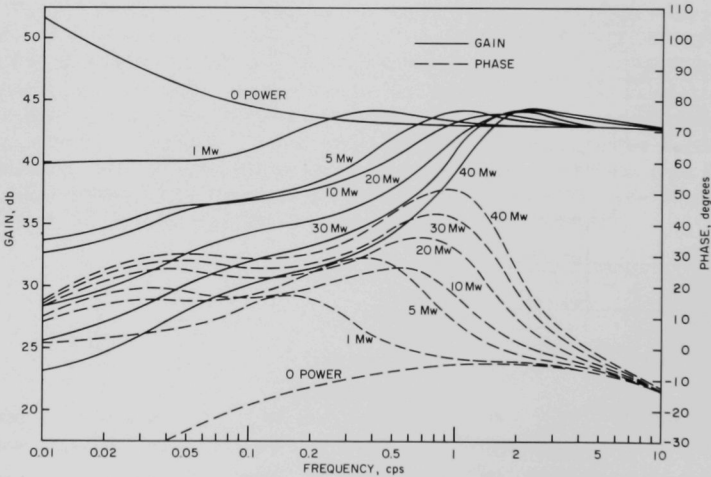


Fig. 14.3. Calculated Transfer Function at Various
Power Levels; Natural Convection; Void
Coefficient: $3.0 \times 10^{-3} \Delta k / \% \text{ Void}$

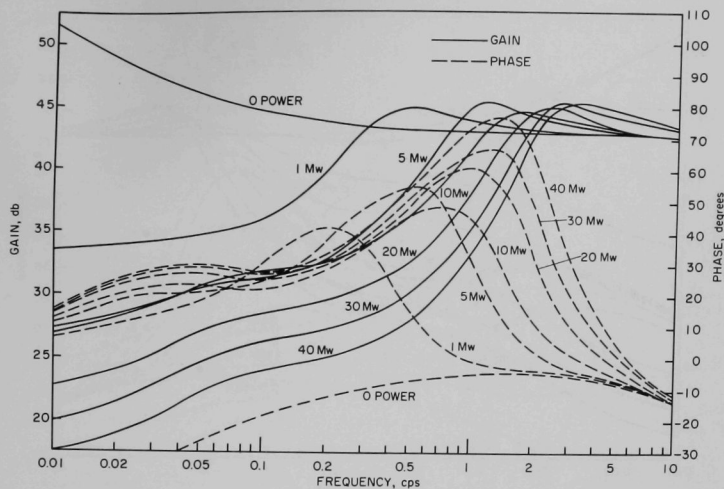


Fig. 14.4. Calculated Transfer Function at Various Power Levels; Natural Convection; Void Coefficient: $4.5 \times 10^{-3} \Delta k/\% \text{ Void}$

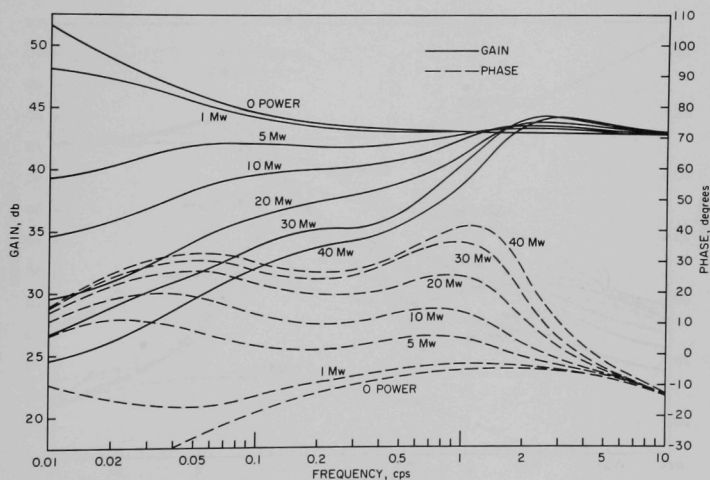


Fig. 14.5. Calculated Transfer Function at Various Power Levels; Forced Convection; 10,000 gpm; Void Coefficient: $3.0 \times 10^{-3} \Delta k/\% \text{ Void}$

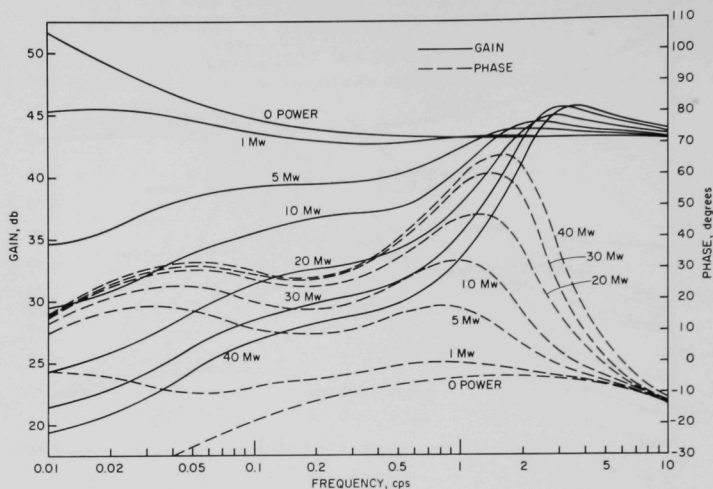


Fig. 14.6. Calculated Transfer Function at Various Power Levels; Forced Convection; 10,000 gpm; Void Coefficient: $4.5 \times 10^{-3} \Delta k/\gamma\%$ Void

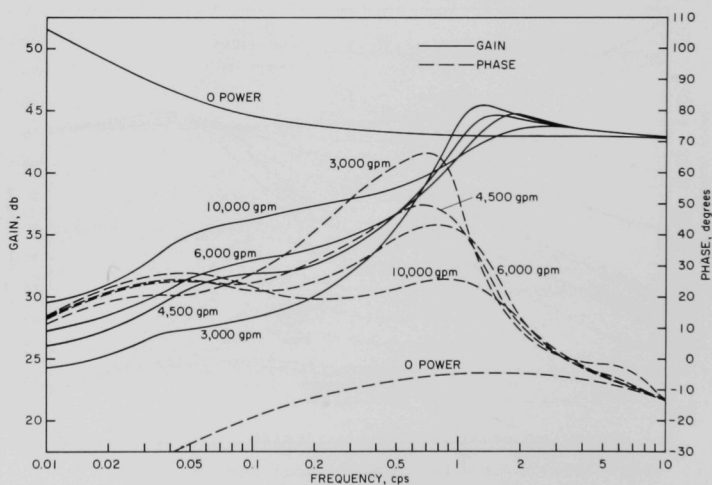


Fig. 14.7. Calculated Transfer Function at Various Flow Rates; Forced Convection; 20 MW; Void Coefficient: $3.0 \times 10^{-3} \Delta k/\gamma\%$ Void

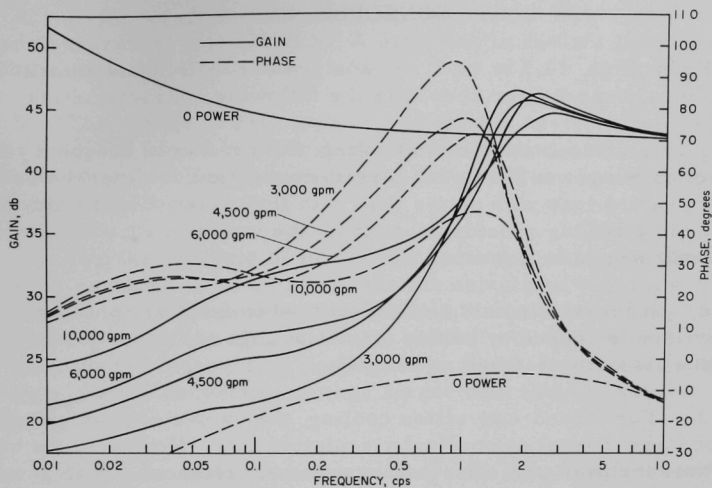


Fig. 14.8. Calculated Transfer Function at Various Flow Rates; Forced Convection; 20 MW; Void Coefficient: $4.5 \times 10^{-3} \Delta k/\% \text{ Void}$

CONCLUSIONS

From Figs. 14.3 to 14.8, the analytical results show that BORAX-V, with a central superheater core, has the following characteristics:

1. In natural-convection cooling, the resonance frequency is highly dependent on the power level; for forced-convection cooling, the resonant frequency varies less with power than with flow rate. Usually the resonance frequency of a boiling reactor depends on the void transit time, so that the above result should be expected.

2. Increases in void coefficient tend to decrease stability. Since the resonance is caused by bubble formation lags in the feedback, this result was also expected before analysis.

3. For forced-convection cooling, the values of peak gain increase with mean power level at constant circulation rate. However, for natural circulation, the peak gain does not increase monotonically with power as it does in forced convection. The results show, for example, that the 5-MW peak is higher than that at 10 MW, while for power levels greater than 10 MW, the peak gain for the natural-convection case increases with power. The latter can be explained by the following effects:

- (a) Figure 14.1 shows that the steady-state water-circulation rate decreases very rapidly as the steady-state power is decreased below 10 MW. The assumed extrapolation shows that slip ratio also decreases with decreasing power level. For example, the water circulation rate at 5 MW is less than half the value at 10 MW. Similarly, the values of slip ratio at 5 and 10 MW are calculated (extrapolated) to be 1.4 and 2.0, respectively. For the above reasons, the power-void, power-boiling boundary, and the boiling boundary-void transfer functions are nearly identical in the range from 5 to 10 MW.

- (b) The part of the feedback loop that is affected, however, as power is increased from 5 to 10 MW is composed of the following two parts: (1) the pressure-boiling boundary transfer function, and (2) the boiling boundary-void transfer function. The product of the above two transfer functions was found to have a much larger gain and somewhat higher phase lag at 5 MW than at 10 MW. Thus, the indicated effects of power level on peak gain of the overall transfer function at the lower power levels for the natural convection case can be summarized as follows: The dynamic results depend heavily on the steady-state model assumed. It is admitted that the calculated steady-state results had to be extrapolated at the lower power levels (below 10 MW), which gave rise to the effects described above.

4. In forced-convection cooling, the coolant flow rate is one of the important factors for stability. A decrease in coolant flow rate tends to decrease stability.

5. The values of peak gain at high-power operation are not too different from the cases of natural-convection cooling and 10,000 gpm forced-convection cooling at equal power levels. The reason for this can be explained as follows:

For the analysis of forced-convection cooling, the calculated slip ratio is assumed to be smaller than the calculated slip ratio for natural convection at high power levels. Hence, in this analysis, the void volume inside the core is not too different from natural-convection cooling and 10,000-gpm, forced-convection cooling. The water-flow velocity for 10,000-gpm, forced convection is thus larger than that for natural convection.

In the analysis, the effects due to the small differences in the void volume in the core and the large difference in the water temperature in the core cancel each other for the case of natural-convection cooling and 10,000-gpm, forced-convection cooling.

In actuality, the slip ratio is not constant for forced convection, but may increase with operating power. The resonance peak value would thus decrease, and resonance frequency would increase when compared with the analytical results for the case of 10,000-gpm, forced convection presented herein.

The object of this analysis was to estimate the stability of BORAX-V with a central superheater core before actual operation. Analytical results show that BORAX-V with a central superheater core will have stable characteristics under the designed operating conditions of power, pressure, and flow.

ACKNOWLEDGMENT

The author gratefully acknowledges the discussions with and suggestions made by F. W. Thalgott, R. E. Rice, D. H. Shaftman, R. A. Cushman, and Dale Mohr. Special thanks are due to H. Nakamura who wrote the transfer-function calculating code for the IBM-1620.

REFERENCES

1. D. H. Crimmins, D. Mohr, and J. T. Stone, Pathfinder Atomic Power Plant Analog Simulator, ACNP-62001 (1962).
2. A. Ziya Akcasu, Theoretical Feedback Analysis in Boiling Water Reactors, ANL-6221, October 1960.
3. J. A. DeShong, Jr., and W. C. Lipinski, Analyses of Experimental Power-Reactivity Feedback Transfer Function for a Natural Circulation Boiling Water Reactor, ANL-5850, July 1958.
4. R. A. Cushman, Calculation of the Natural Convection Flow on the BORAX-V, unpublished.
5. Design and Hazards Summary Report, Boiling Reactor Experiment V (BORAX-V), ANL-6302, May 1961.

SUPPLEMENTARY REFERENCES

- S. Hayashi, T. Iwazumi, J. Wakabayashi, A. Sakurai, and M. Kitamura, Experimental Study on Temperature Overshoot and Delay Time of Transient Boiling, J. of Atomic Energy Society, Japan, 2-736 (1960).
- J. B. Heineman, An Experimental Investigation of Heat Transfer to Superheated Steam in Round and Rectangular Channels, ANL-6213, September 1960.
- Paul A. Lottes, Nuclear Reactor Heat Transfer, ANL-6469, December 1961.

ARGONNE NATIONAL LAB WEST



3 4444 00009086 0